

Vacancy-induced enhancement of magnetic interactions in (Ca, Na)-doped lanthanum manganites

A. I. Tovstolytkin,^{a)} A. M. Pogorily, and D. I. Podyalovskii

Institute of Magnetism of the NAS of Ukraine, 36-b Vernadskogo Str., Kyiv 03142, Ukraine

V. M. Kalita, A. F. Lozenko, P. O. Trotsenko, and S. M. Ryabchenko

Institute of Physics of the NAS of Ukraine, 46 Nauki Pr., Kyiv 03028, Ukraine

A. G. Belous, O. I. V'yunov, and O. Z. Yanchevskii

Institute of General and Inorganic Chemistry of the NAS of Ukraine, 32/34 Palladina Pr., Kyiv 03142, Ukraine

(Received 25 April 2007; accepted 22 July 2007; published online 19 September 2007)

Structural, electric, and magnetic properties of the bulk polycrystalline samples with nominal composition $\text{La}_{0.7}\text{Ca}_{0.3-x}\text{Na}_x\text{MnO}_3$ ($x=0-0.10$) have been investigated in the work. As follows from the results of chemical and x-ray structural analyses, the increase in x brings about the rise in the number of structural vacancies in both lanthanum and oxygen sublattices. The influence of the variation of the vacancy number on peculiar features of the transition from ferromagnetic metallic state to paramagnetic state with activated conductivity has been studied in detail. The conclusion is made that the rise in the number of structural vacancies gives rise not only to the enhancement of magnetic inhomogeneity and broadening of the magnetic transition, but also to the increase in the temperature of magnetic transition. It is demonstrated that the changes in magnetic parameters also result in the increase of the temperatures of resistivity and magnetoresistance peaks as well as in the change of the character of the temperature dependence of electric resistance. © 2007 American Institute of Physics. [DOI: 10.1063/1.2778738]

I. INTRODUCTION

In recent years, the doped lanthanum manganites $\text{La}_{1-x}\text{M}_x\text{MnO}_3$, where M is an ion of alkaline or alkaline-earth element, have attracted a great deal of research interest due to a number of unusual physical properties, including in particular colossal magnetoresistance effect (CMR).^{1,2} The essence of the CMR phenomenon consists in an abrupt increase in electric resistance under the influence of an external magnetic field. Mainly due to this effect the doped manganites are considered promising materials for elaboration of new generation of magnetic sensors and devices of the magnetic information readout.^{3,4}

At the same time, numerous experimental studies have revealed complex combinations of structural, magnetic, and electronic properties of manganites, which, being interesting from the physical point of view, have not found a satisfactory explanation yet.⁵ The complexity of electronic and magnetic phase diagrams of doped manganites results from a strong interaction among the charge, spin, and orbital subsystems, in which manganese ions play a key role.³⁻⁵ The interference between these systems is also the reason for the strong sensitivity of electric properties of manganite materials to their magnetic and structural peculiarities.

The doping, stoichiometry, disorder, and strain collectively determine the properties of CMR manganites. In such a complex situation there is some attraction in attempting to use averaged values of parameters such as oxidation state of manganese ions, ionic radius in lanthanum sublattice, Mn–O

distance, and Mn–O–Mn bond angle to explain the observed trends in the Curie temperature, T_C , and electric and magnetoresistive properties.⁵⁻⁷ At present, it is considered as reliably established that the magnetic state and electric properties of $\text{La}_{1-x}\text{M}_x\text{MnO}_3$ compounds are mainly governed by three parameters: (i) the concentration of charge carriers, which depends on the mean oxidation state of manganese ions; (ii) the average radius of ions in lanthanum sublattice; and (iii) the degree of disorder caused by a radius mismatch in La sublattice.³⁻⁷ Although there are many examples demonstrating apparently systematic trends, it is obvious that these averaged quantities mask the effects arising from a different degree of deviation of a real quantity from the averaged one. To specify these effects, it is necessary to carry out additional investigations on a series of carefully prepared and characterized samples with fixed values of averaged parameters.

The lanthanum manganite compounds doped with sodium or potassium seem to be the particularly appropriate objects to achieve this aim. The point is that the strong volatility of sodium (potassium) at high temperatures gives rise to the formation of vacancies in the lanthanum sublattice and it turns out that the larger the number of vacancies, the higher the concentration of sodium in the starting charge is.⁸⁻¹¹ In prevailing cases this results in the fact that for samples with a starting composition $\text{La}_{1-x}(\text{Na},\text{K})_x\text{MnO}_3$, the increase in x leads only to negligible changes in the oxidation state of manganese ions. What is more, in most cases, is that the average crystallographic parameters remain practically constant for a sufficiently wide range of x ($0 \leq x \leq 0.3$).^{8,10,11} Therefore, the investigation of well-

^{a)}Corresponding author: atov@imag.kiev.ua

characterized Na-doped perovskite manganites gives birth to hopes of isolating the effects caused exclusively by the increase in the number of vacancies, holding at the same time the rest of the averaged parameters nearly constant.

The effect of structural vacancies on magnetic and electric properties of $\text{La}_{1-x}\text{M}_x\text{MnO}_3$ compounds has been studied in a number of papers.^{10–20} In most cases, the results agree with each other in the fact that the increase in the number of vacancies brings about a rise in resistivity and broadening of magnetic transitions. Both of these effects are thought to result from the enhancement of material inhomogeneity.^{12,13,17–19} However, to date, there are no consistent views concerning the vacancy effect on other parameters of CMR manganites. This partly results from the fact that in almost all the works, the change in the number of vacancies leads simultaneously to the change in crystallographic parameters and manganese oxidation state, which did not allow the authors to isolate the effect of structural vacancies in pure form.

The aim of this work is to specify the regularities of the influence of the change in the number of structural vacancies on magnetic, electric, and magnetoresistive parameters of the polycrystalline samples of $\text{La}_{0.7}\text{Ca}_{0.3-x}\text{Na}_x\text{MnO}_3$ (LCNM) system.

II. DETAILS OF EXPERIMENT

The samples with a nominal chemical composition $\text{La}_{0.7}\text{Ca}_{0.3-x}\text{Na}_x\text{MnO}_3$ ($x=0, 0.04, 0.06, 0.08$, and 0.10) were prepared by solid-state reactions using appropriate mixtures of extra purity grade La_2O_3 and Mn_2O_3 , and reagent grade CaCO_3 and Na_2CO_3 . The stoichiometric amounts of dehydrated reagents were mixed and homogenized by vibration milling for 6–8 h in distilled water with corundum grinding media. Then, the mixtures were dried at $100\text{--}120^\circ\text{C}$ and passed through a nylon 6 sieve. After preliminary annealing ($920\text{--}960^\circ\text{C}$, 4 h), wet homogenizing millings were repeated. After addition of an aqueous solution of polyvinyl alcohol as a binder, the powder was pressed into disks 10 mm in diameter and 3–4 mm in thickness, which were then sintered at 1200°C for 4 h.

X-ray diffraction (XRD) measurements were made on a DRON–4–07 powder diffractometer (Cu $K\alpha$ radiation). Crystallographic parameters and phase composition were determined by the Rietveld profile analysis method using the FULLPROF program and PDF-2 Software of the International Centre for Diffraction Data (ICDD). XRD patterns were run in the angular range $2\theta=10^\circ\text{--}150^\circ$ in a step-scan mode with a step size of 0.02° and a counting time of 10 s per data point. As the external standards, SiO_2 (2θ calibration) and Al_2O_3 (NIST SRM1976 intensity standard) were used. The Mn^{3+} and Mn^{4+} contents were determined by titration with an iodine thiosulfate solution. The iodine in the potassium iodide solution was replaced by chlorine resulting from the dissolution of a manganite sample in hydrochloric acid. Inaccuracy in determination of a fraction of Mn^{4+} ions did not exceed 2%. Na content was determined by the method of atomic absorptive spectroscopy, in which inaccuracy in the given case did not exceed 6%.

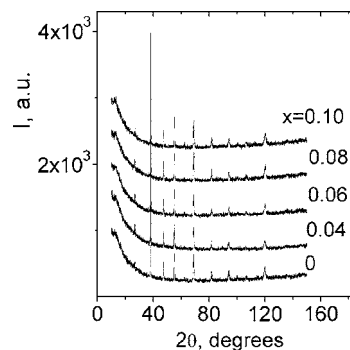


FIG. 1. XRD patterns for LCNM samples with various x .

The measurements of electric resistance were carried out by a four-probe method in the temperature range of $77\text{--}400\text{ K}$. The specimens for these measurements were cut rectangular in shape, $2 \times 3 \times 10\text{ mm}^3$ in dimensions. Electric contacts were made by firing silver paste. Magnetoresistance, MR , was measured in fields up to 15 kOe and was determined as $(\rho - \rho_H)/\rho$, where ρ is resistivity in zero magnetic field, and ρ_H is resistivity in the external field H .

Magnetostatic measurements were performed in the temperature range $120\text{--}500\text{ K}$ using a LDJ-500 vibrating sample magnetometer. Electron spin resonance (ESR) measurements were carried out with the use of an X-band electron paramagnetic resonance (EPR) spectrometer (Radiopan SE/X-2544; operating frequency $\nu \cong 9.2\text{ GHz}$). The samples for the ESR investigations were grinded into a powder with the grains a few microns in size.

III. RESULTS OF EXPERIMENTS

A. Structure and chemical composition

XRD patterns for LCNM samples with various x are plotted in Fig. 1. As follows from the analysis of the data, all the samples are single phase and characterized by a rhombohedrally distorted perovskite structure (the $R\bar{3}c$ space group). Crystallographic parameters obtained by means of Rietveld refinement are shown in Table I. It is seen that the increase in x does not lead to any noticeable changes in the lattice parameters or volume of elementary cell: the change in each of the parameters does not exceed 0.5% as x grows from 0 to 0.10. Such data agree well with the results of the majority of papers devoted to the study of sodium (potassium)-doped lanthanum manganites.^{8,10,11}

To estimate the degree of defectiveness for the samples under investigation, we carried out a series of the chemical analyses which made it possible to determine the actual sodium content and atomic fractions of Mn^{3+} and Mn^{4+} ions. As a result, the actual chemical composition was established for all the samples synthesized (Table II). It is evident that both the absolute and relative losses of sodium, incurred in the process of synthesis, are greater for the samples which contain more sodium in a starting charge. However, the increase in x leads not only to the rise in the number of vacancies in the lanthanum sublattice, but also to the change in the oxygen nonstoichiometry parameter γ . So, γ decreases from 0.033 to -0.0685 upon the growth in x from 0 to 0.10. As a

TABLE I. Crystallographic parameters for the LCNM samples.

Parameters	x				
	0	0.04	0.06	0.08	0.10
Lattice parameters					
a , Å	5.474(3)	5.473(2)	5.469(3)	5.471(3)	5.472(1)
c , Å	13.376(7)	13.363(7)	13.366(7)	13.365(5)	13.346(4)
c/a	2.4435	2.4442	2.4439	2.4425	2.4393
V , Å ³	347.1(3)	346.3(3)	346.2(3)	346.3(2)	346.0(2)
Some distances and angles					
Mn–O, Å	1.953(5)	1.955(3)	1.956(6)	1.956(6)	1.955(4)
Mn–O–Mn, degrees	163.9(13)	162.2(5)	163.2(13)	162.4(12)	162.3(9)
Discrepancy factors					
R_B , %	11.7	11.9	10.5	12.9	10.9
R_F , %	11.2	9.48	8.83	11.3	12.3

result of such changes, the fraction of Mn^{4+} ions decreases from 0.363 to 0.315. It is noteworthy that such trends agree well with those observed in Ref. 8, where a careful investigation and chemical analysis of the samples $\text{La}_{1-x}\text{A}_x\text{MnO}_3$ ($\text{A}=\text{Na}$, K , Rb , and Sr) was performed.

B. Electric and magnetoresistive properties

Figure 2(a) shows the temperature dependence of resistivity ρ in the temperature range 77–400 K. For the sample with $x=0$, the ρ vs T dependence exhibits a sharp maximum at a temperature $T_p \cong 273$ K. It should be noted that both the character of $\rho(T)$ dependence and the value of T_p agree with what was obtained by other researchers on $\text{La}_{1-x}\text{Ca}_x\text{MnO}_3$ polycrystalline samples with $x \sim 0.3$.^{3–5,21,22}

A change in x gives rise to the changes in both the character of $\rho(T)$ curves and values of T_p and ρ_{max} , where ρ_{max} is the maximal value of ρ in the temperature range under investigation. As the content of sodium grows, ρ_{max} first increases from 0.2 Ω cm ($x=0$) to ~ 3 Ω cm ($x=0.06$) and then slightly decreases, reaching ~ 2 Ω cm in the sample with $x=0.10$. For the samples with $x \neq 0$, an additional broad peak emerges on the $\rho(T)$ dependences in the low-temperature region ($T < T_p$). It becomes more pronounced with the x growth, whereas the peak at T_p gets less noticeable and eventually turns into an inconspicuous kink. The value of T_p determined as a temperature of the kink on $\rho(T)$ curves increases with x growing and reaches 303 K in LCNM with $x=0.10$.

It is known that in doped manganites the maximum on $\rho(T)$ dependence is related to the transition from a ferromag-

netic phase with metallic ($d\rho/dT > 0$) conductivity to a paramagnetic one with activated conductivity ($d\rho/dT < 0$). In single crystals, the value of T_p is close to the ferromagnetic to paramagnetic transition temperature T_C ,^{3–5} but what is often observed in polycrystals and inhomogeneous manganites is either a broadened maximum near T_C or two peaks, with the second one being located in the low-temperature region.^{15,23} The reason for the appearance of the second peak still remains controversial, but most often it emerges in highly inhomogeneous materials.^{15,23} In our case, the fact that the width and intensity of the low-temperature peak increase with the increase in x testifies to the enhancement of the samples' inhomogeneity. Such behavior is consistent with the results of the chemical analysis, which shows that the increase in x gives rise to the increase in the number of vacancies.

Figure 2(b) shows the temperature dependences of magnetoresistance measured in field $H=15$ kOe. According to the literature data,^{3,4,24–26} magnetoresistance in the single crystals of doped manganites displays a maximum near Curie point T_C and drops as the temperature deviates from T_C . In polycrystalline samples, however, an additional contribution to MR is observed in the low-temperature region, which monotonously rises with temperature lowering.^{24–27} The appearance of the additional contribution is shown to be associated with the spin-dependent transfer of charge carriers through intergrain regions.^{24–26} In all the samples under study, both contributions to magnetoresistance are well discernable. It is noteworthy that the low-temperature contribution to MR is almost the same for all the samples, but the

TABLE II. The actual composition of the LCNM samples as results from a series of chemical analyses. x_{real} : the real content of sodium. A/B : the ratio between the occupancies of lanthanum and manganese sublattices. (\square) denotes the vacancy in the lanthanum sublattice. Parameter γ characterizes the deviation of oxygen content from the stoichiometric value.

x	x_{real}/x	$\text{Mn}^{4+}/(\text{Mn}^{4+} + \text{Mn}^{3+})$	A/B	γ	Actual composition
0		0.363	1	+0.033	$\text{La}_{0.7}\text{Ca}_{0.3}\text{MnO}_{3.033}$
0.04	0.78	0.335	0.9912	−0.007	$\text{La}_{0.7}\text{Ca}_{0.26}\text{Na}_{0.0312}\square_{0.0088}\text{MnO}_{2.993}$
0.06	0.79	0.331	0.9874	−0.0208	$\text{La}_{0.7}\text{Ca}_{0.24}\text{Na}_{0.0474}\square_{0.0126}\text{MnO}_{2.9792}$
0.08	0.54	0.323	0.9632	−0.0469	$\text{La}_{0.7}\text{Ca}_{0.22}\text{Na}_{0.0432}\square_{0.0368}\text{MnO}_{2.9531}$
0.10	0.475	0.315	0.9480	−0.0685	$\text{La}_{0.7}\text{Ca}_{0.20}\text{Na}_{0.0480}\square_{0.0520}\text{MnO}_{2.9315}$

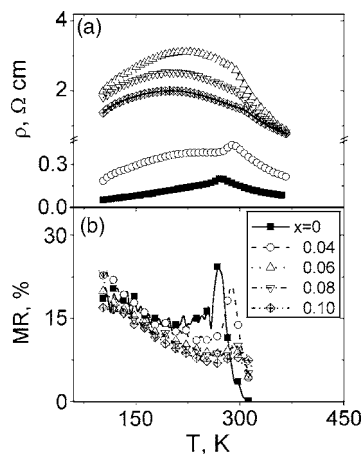


FIG. 2. Temperature dependences of resistivity ρ (a) and magnetoresistance MR (b) for LCNM samples.

high-temperature peak undergoes drastic transformations: the MR peak shifts toward higher temperatures and decreases with the increase in x .

C. Magnetic properties

Figure 3 shows the magnetization M versus magnetic field H dependences for LCNM with $x=0$, 0.04, and 0.08, obtained at 120 K (the lowest temperature achievable in our measurement setup) by means of a cyclic change of field from -10 to 10 kOe and backward. The shape of $M(H)$ curves is indicative of the presence of ferromagnetic ordering. With the increase in H , the magnetization first sharply grows, then the growth gets slower, and magnetization saturates as the field exceeds ~ 4 kOe. As seen from the figure, all curves are very close to each other. The saturation magnetization M_S is reduced from 88 to 80.1 emu/g as x grows from 0 to 0.10. There is a hysteresis in the low-field (<500 Oe) region (see inset of Fig. 3). The coercivity is almost independent of x and does not exceed 55 Oe.

To analyze the behavior of LCNM samples in the vicinity of the transition from ferromagnetic to paramagnetic state, the $M(H)$ isotherms were replotted in the form $M^2(H/M)$, the so-called Arrott-Belov plots.^{28,29} Such plots are used for a detailed analysis of the behavior of magnetically ordered materials in the vicinity of magnetic transition and for determination of the Curie temperature.^{28,29} Intersection of the linear asymptote, coinciding with an Arrott-Belov plot at high fields, with the M^2 axis, allows the determination of spontaneous magnetization $M_0(T)$ at temperatures below

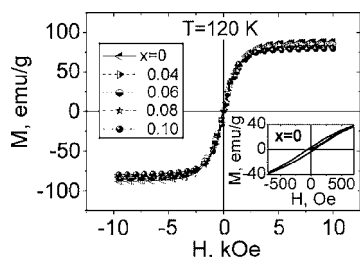


FIG. 3. Magnetization curves $M(H)$ for LCNM samples. The inset shows the hysteresis loop in the low-field region for the sample with $x=0$.

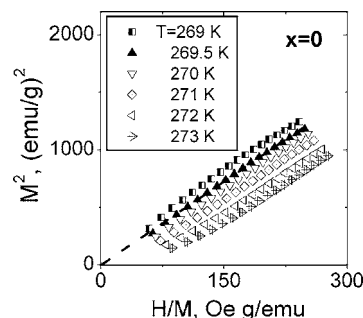


FIG. 4. Dependences M^2 vs H/M in the vicinity of the ferromagnetic to paramagnetic transition for LCNM with $x=0$.

the magnetic transition point. The temperature at which the asymptote to the $M^2(H/M)$ curve passes through the coordinate origin is thought to be the actual Curie temperature.

Figures 4 and 5 show the $M^2(H/M)$ curves for two LCNM samples. For the sample with $x=0$, the temperature of magnetic transition T_C^A determined from the Arrott-Belov plots is equal to 269.5 K. The samples with a higher level of sodium content display greater values of T_C^A . So, T_C^A equals 276 and 289 K for the samples with $x=0.04$ and 0.08, respectively.

D. Resonance properties

A peculiar feature of ESR spectra for all the samples under investigation is a coexistence of two absorption lines over a wide temperature range. As an example, the temperature evolution of magnetic resonance spectra for LCNM with $x=0.04$ is presented in Fig. 6. In a high-temperature region ($T > 305$ K), the spectrum consists of a single symmetric line. The integrated curve is well described by a Lorentzian with parameters that correspond to the paramagnetic state of manganites (resonance field $B_r \approx 310$ mT, linewidth $w_{pp} \approx 25$ mT). As the temperature is reduced, an additional signal with a lower resonance field emerges, which corresponds to ferromagnetic phase. The further decrease in temperature gives rise to a substantial enhancement of the intensity of the ferromagnetic resonance line concomitant with the weakening of the signal from the paramagnetic phase, until the latter completely disappears.

As follows from the analysis of the ESR spectra, the signal from the ferromagnetic phase emerges at temperatures well exceeding the values of T_C^A obtained from the Arrott-Belov plots. In particular, for the sample with $x=0.04$, T_C^A

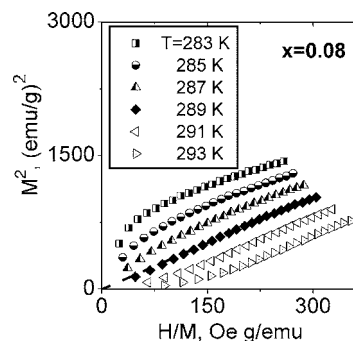


FIG. 5. The same as in Fig. 4 for LCNM with $x=0.08$.

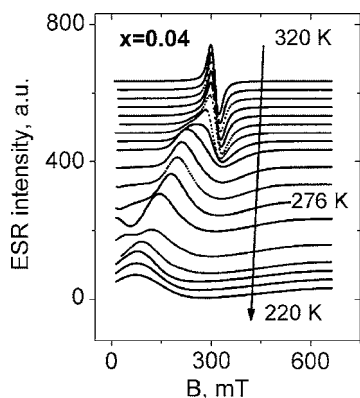


FIG. 6. ESR spectra for LCNM with $x=0.04$ measured at various temperatures.

≈ 276 K. However, as follows from the analysis of the resonance data, the ESR spectrum at this temperature contains signals from both the ferromagnetic and paramagnetic phases.

To make a quantitative estimation of the parameters of the ESR spectra, the following procedure was used. The temperature, at which the root-mean-square deviation of the ESR line data from Lorentzian exceeds 5%, was denoted as T_0 and the parameter $\Delta T = T_0 - T_C^A$ was used to characterize the width of magnetic transition. The analysis of the data obtained shows that the increase in x in the LCNM samples leads to the increase in both T_0 and Δ values.

IV. ANALYSIS OF RESULTS

Magnetic properties of $\text{La}_{1-x}\text{M}_x\text{MnO}_3$ compounds are for the most part governed by the exchange interactions between the magnetic moments of manganese ions.³⁻⁵ At the heart of such interactions lies a virtual or real transfer of electrons through the oxygen ions. If manganese ions are in Mn^{3+} and Mn^{4+} states, the interaction, which is based on a simultaneous transfer of one electron from a d orbital of Mn^{3+} to an oxygen p orbital, and another one from an oxygen p orbital to an empty d orbital of a neighboring Mn^{4+} , dominates in the CMR manganites.¹⁻⁵ Such mechanism, referred to as double exchange, favors ferromagnetic ordering and is the principal mechanism of electric conductivity in doped manganites in the low-temperature region. It is clear that the efficiency of the double exchange depends on the ratio between Mn^{3+} and Mn^{4+} ions, i.e., the average oxidation state of manganese ions, as well as on the degree of overlap between manganese d orbitals and oxygen p orbitals, i.e., the crystallographic and microstructural parameters.

As was noted in the Introduction, to find the tools to govern the electric, magnetic, and magnetoresistive properties of the perovskite manganites, the averaged values of a number of parameters, such as oxidation state of manganese ions, ionic radius in lanthanum sublattice, Mn–O distance, and Mn–O–Mn bond angle, are widely used. Let us show that the data we obtained in this paper cannot find a satisfactory explanation within the framework of such an approach.

Estimate the influence of structural factors from the following considerations. As was shown in Ref. 30, the hydrostatic pressure leading to 1% strain changes the Curie tem-

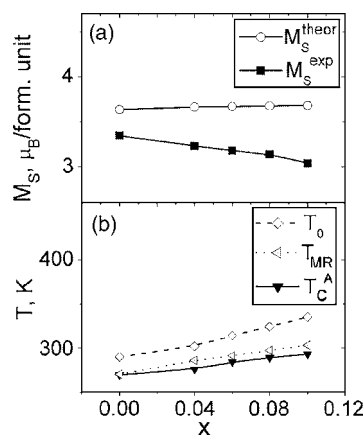


FIG. 7. (a) Concentration dependence of the saturation magnetization obtained experimentally (M_S^{exp}) and calculated theoretically (M_S^{theor}). (b) Concentration dependence of T_0 , T_{MR} , and T_C^A for LCNM samples.

perature of $\text{La}_{2/3}\text{Ca}_{1/3}\text{MnO}_3$ polycrystalline samples by about 10 K. In our case, as follows from the results of structural investigations (see Sec. III A), the changes in averaged crystallographic parameters do not exceed 0.5% as x grows from 0 to 0.10. Therefore, the change in T_C caused by the variation of structural parameters should not exceed ~ 5 K.

The analysis of the changes in the mean oxidation state of manganese ions leads to similar conclusions. It is known that the efficiency of double exchange is maximal when the fraction of Mn^{4+} equals 33% of the total number of manganese ions.³⁻⁵ In the vicinity of this value the 2%–3% deviation of the Mn^{4+} fraction to either side of the temperature scale can only lead to very small variations in T_C and only toward its diminution. In our case, as is seen from the results described in Secs. III C and III D, the values of T_C^A and T_0 rise by 8 and 13%, respectively, as x changes from 0 to 0.10. The same trend is also characteristic of the behavior of the temperatures of the peaks on $MR(T)$ and $R(T)$ curves.

Analyzed in more detail are the magnetic properties of LCNM samples. Figure 7(a) shows the concentration dependence of the saturation magnetization M_S^{exp} obtained experimentally at 120 K. In the same graph we also plotted $M_S^{\text{theor}}(x)$ dependence calculated under the assumption that all the manganese ions are ordered ferromagnetically. The values of both quantities are plotted in Bohr magnetons per formula unit. It is evident that for all the samples under discussion, M_S^{exp} is by 8%–17% smaller than M_S^{theor} . Therefore, not all the volume of the samples is in ferromagnetic state. As one can reasonably expect, it is the regions near the structural imperfections (vacancies, intergrain boundaries, and others) that remain magnetically disordered down to the lowest temperatures. The value of M_S^{exp} decreases with the increase in x , which is in compliance with the data testifying to the increased number of vacancies in the samples with a higher level of sodium doping.

As was noted above, to the effects which result from the increase in the number of structural vacancies belong the enhancement of magnetic inhomogeneity and broadening of magnetic transition. Let us consider from this point of view the data that we obtained. To analyze the behavior of the magnetic parameters of LCNM samples, we plotted the con-

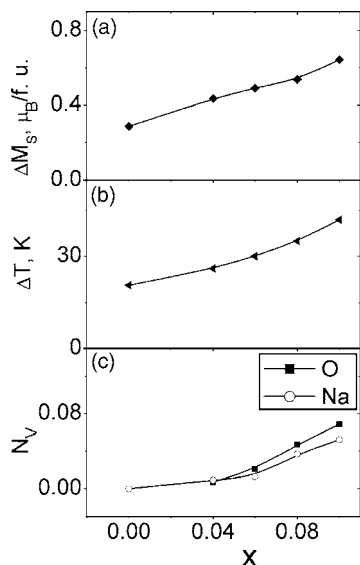


FIG. 8. Concentration dependences of (a) ΔM_S , (b) ΔT , and (c) the number of vacancies N_V in LCNM samples.

centration dependences of $\Delta M_S = M_S^{\text{theor}} - M_S^{\text{exp}}$ and $\Delta T = T_0 - T_C^A$ [Figs. 8(a) and 8(b)]. The former parameter can be used to estimate the degree of magnetic inhomogeneity of the samples in the low-temperature region, and the latter to characterize the magnetic transition width. The same figure also shows the concentration dependence of the number of vacancies in the lanthanum and oxygen sublattices [Fig. 8(c)]. As seen from the figure, all the dependences correlate well with each other, which can serve as a quantitative confirmation of the statement about enhancement of magnetic inhomogeneity with the increase in the number of structural vacancies.

Figure 7(b) shows the concentration dependences of characteristic temperatures, which reflect the peculiar features of the transition from ferromagnetic to paramagnetic state. The values of these temperatures are obtained from the analysis of different physical quantities and characterize various sides of the magnetic transition in LCNM samples. T_0 is the temperature at which, according to the ESR data, the ferromagnetic phase is nucleated, whereas the paramagnetic one still remains dominating. As temperature is lowered, more and more volume fraction of a sample turns into the ferromagnetic state and magnetization reaches a value which becomes measurable with the use magnetometry methods. Apparently T_C^A , obtained from the analysis of Arrott-Belov plots, characterizes just this temperature.

As was noted above, in doped manganites the charge transfer between manganese ions strongly depends on the mutual orientation of their magnetic moments. The effectiveness to order magnetic moments by means of the external magnetic field is maximal near the temperature of the transition to ferromagnetic phase. However, the contribution of the regions, where the ferromagnetism is nucleated, to the resistance and magnetoresistance will be noticeable only under the conditions that the fraction of these regions is not negligibly small but constitutes a sizeable part of the volume of the sample. It is this fact to which testifies the proximity of the temperature T_{MR} , at which magnetoresistance reaches a maximum, to T_C^A [see Fig. 7(b)]. It is noteworthy that the

appearance of the difference between the values of T_0 , T_{MR} , and T_C^A is considered as natural for the strongly broadened transitions.

As seen from Fig. 7(b), the values of T_0 , T_{MR} , and T_C^A increase by more than 13% as x grows from 0 to 0.10. It was shown above that neither the changes in the average oxidation state of manganese nor the variations of the structural parameters (not exceeding 0.5%), which are observed in LCNM samples, can lead to a noticeable change in the Curie temperature, especially to its growth. At the same time, a comparison of Figs. 7(b) and 8(c) allows one to notice a correlation between the variation of the temperatures, which characterize the magnetic transition, and the change in the number of structural vacancies in LCNM samples, and relate the rise of the temperature of magnetic transition to the increase in the number of vacancies.

The mechanism of influence of structural vacancies on the parameters of magnetic transition can be as follows. The translation symmetry, inherent to crystalline materials, imposes serious limitations on both the number of nearest neighbors of a chosen ion and the distance between the neighboring ions. For this reason, the ideal crystal is expected to be characterized by a weak deviation of these quantities from the averaged values. Since these quantities determine the efficiency of the exchange interaction, one should expect that the spread of magnetic characteristics such as magnetization and Curie temperature is sufficiently small.

A partial breaking of the translational symmetry, in particular by means of the formation of structural vacancies, gives rise to the introduction of disorder into the ion arrangement and, therefore, to the increase in the scatter of the values of magnetic parameters, which, in turn, can lead to the appearance of the spatial inhomogeneity in magnetization and to the broadening of magnetic transition. Such effects were observed by us in this work and were also reported by other research groups.^{16–20} However, the introduction of structural imperfections can also remove the limitations imposed by translational symmetry on the arrangement of neighboring ions and lead to those configurations which favor the enhancement of exchange interactions. Apparently it is this situation that occurs in our case.

It should be noted that the effect of the Curie temperature growth upon the increase in the number of vacancies was also observed in a number of papers,^{11,18,20,31} and most often it was interpreted as originating from the variation of averaged oxidation state of manganese. Such explanation is valid and well grounded for the case of the variation of the number of structural vacancies in the lanthanum sublattice. However, the situation is not so unambiguous in other cases, in particular when there are vacancies in both anionic and cationic sublattices. This fact was stressed in Ref. 8, where a careful investigation and chemical analysis of the samples $\text{La}_{1-x}\text{A}_x\text{MnO}_3$ ($\text{A} = \text{Na, K, Rb, and Sr}$) was performed and the authors came to conclusions similar to ours.

V. CONCLUSIONS

In this work, we have specified the regularities of the changes in electric, magnetoresistive, and resonance proper-

ties upon a variation in the number of structural vacancies in the $\text{La}_{0.7}\text{Ca}_{0.3-x}\text{Na}_x\text{MnO}_3$ ($x=0\div 0.10$) doped manganites. It is shown that the growth of x gives rise to the increase in the number of vacancies in both the lanthanum and oxygen sublattices. At the same time, the variation of the averaged crystallographic parameters (the lattice parameters and the volume of elementary cell, Mn–O interionic distance, and Mn–O–Mn bond angle) does not exceed 0.5% and the fraction of the fourfold ionized manganese ions decreases from 36.3% to 31.5%, which, according to currently prevailing views, should not bring about the variation of the magnetic state of the samples. For all samples under investigation, the saturation magnetization obtained experimentally is less than that calculated under the assumption that all manganese ions are ordered ferromagnetically. Therefore, not all the sample volume is in the ferromagnetic state. The value of M_S^{exp} decreases with x growing, implying that one of the sources of the appearance of magnetically disordered regions is the rise of structural imperfections, particularly vacancies. The correlation is found between the character of the concentrational changes of the number of vacancies, the degree of magnetic inhomogeneity, and magnetic transition width. It is shown that although the utilization of different methods for the experimental determination of Curie temperature results in different values, for all the cases the transition temperature grows with growing x . It is demonstrated that such change in magnetic parameters results in the increase of the temperatures of resistivity and magnetoresistance peaks as well as in the change of the character of the temperature dependence of electric resistance.

ACKNOWLEDGMENT

The work is partly supported by the Science and Technology Centre in Ukraine, Project No. 3178.

¹R. von Helmolt, J. Wecker, K. Samwer, L. Haupt, and K. Bärner, *J. Appl. Phys.* **76**, 6925 (1994).

²S. Jin, T. H. Tiefel, M. McCormack, R. A. Fastnacht, R. Ramesh, and L. H. Chen, *Science* **264**, 413 (1994).

³A.-M. Haghiri-Gosnet and J.-P. Renard, *J. Phys. D* **36**, R127 (2003).

⁴K. Dörr, *J. Phys. D* **39**, R125 (2006).

⁵E. Dagotto, T. Hotta, and A. Moreo, *Phys. Rep.* **344**, 1 (2001).

⁶H. Y. Hwang, S.-W. Cheong, P. G. Radaelli, M. Marezio, and B. Batlogg, *Phys. Rev. Lett.* **75**, 914 (1995).

⁷L. M. Rodriguez-Martinez and J. P. Attfield, *Phys. Rev. B* **54**, R15622 (1996).

⁸T. Shimura, T. Nayashi, Y. Inaguma, and M. Itoh, *J. Solid State Chem.* **124**, 250 (1996).

⁹R. N. Singh, C. Shivakumara, N. Y. Vasanthacharya, S. Subramanian, M. S. Hegde, H. Rajagopol, and A. Sequeira, *J. Solid State Chem.* **137**, 19 (1998).

¹⁰S. L. Ye *et al.*, *J. Appl. Phys.* **90**, 2943 (2001).

¹¹O. Z. Yanchevskii, A. I. Tovstolytkin, O. I. V'yunov, D. A. Durilin, and A. G. Belous, *Inorg. Mater.* **40**, 744 (2004).

¹²R. Dhahri and F. Halouni, *J. Alloys Compd.* **385**, 48 (2004).

¹³P. Kameli, H. Salamati, G. V. Sudhakar Rao, and F. S. Razavi, *J. Magn. Magn. Mater.* **283**, 305 (2004).

¹⁴A. Das, M. Sahana, S. M. Yusuf, L. Madhav Rao, C. Shivakumara, and M. S. Hegde, *Mater. Res. Bull.* **35**, 651 (2000).

¹⁵J. E. Evetts, M. G. Blamire, N. D. Mathur, S. P. Isaak, B.-S. Teo, L. F. Cohen, and J. L. Macmanus-Driscoll, *Philos. Trans. R. Soc. London, Ser. A* **356**, 1593 (1998).

¹⁶D. C. Kundaliya, A. A. Tulapurkar, R. Pinto, R. Kumar, and R. G. Kulkarni, *Solid State Commun.* **122**, 419 (2002).

¹⁷M. L. Wilson, J. M. Byers, P. C. Dorsey, J. S. Horwitz, D. B. Chrisey, and M. S. Osofsky, *J. Appl. Phys.* **81**, 4971 (1997).

¹⁸W. Boujelben, A. Cheikh-Rouhou, M. Ellouze, and J. C. Joubert, *J. Magn. Magn. Mater.* **242–245**, 662 (2002).

¹⁹V. M. Browning *et al.*, *J. Appl. Phys.* **83**, 7070 (1998).

²⁰W. Boujelben, A. Cheikh-Rouhou, J. Pierre, and J. C. Joubert, *J. Alloys Compd.* **315**, 68 (2001).

²¹S. L. Yuan *et al.*, *Phys. Rev. B* **66**, 172402 (2002).

²²V. M. Loktev and Yu. G. Pogorelov, *Low Temp. Phys.* **26**, 171 (2000).

²³A. I. Tovstolytkin, A. N. Pogorily, and S. M. Kovtun, *Low Temp. Phys.* **25**, 1282 (1999).

²⁴A. Gupta, G. O. Gong, G. Xiao, P. R. Duncombe, P. Lecoeur, P. Trouiloud, Y. Y. Wang, and V. P. Dravid, *Phys. Rev. B* **54**, R15629 (1996).

²⁵H. Y. Hwang, S.-W. Cheong, N. P. Ong, and B. Batlogg, *Phys. Rev. Lett.* **77**, 2041 (1996).

²⁶A. Gupta and J. Z. Sun, *J. Magn. Magn. Mater.* **200**, 24 (1999).

²⁷S. L. Yuan *et al.*, *Solid State Commun.* **127**, 743 (2003).

²⁸S. Chikazumi, *Physics of Ferromagnetism*, 2nd ed. (Oxford University Press, Oxford, 1997).

²⁹V. S. Amaral, J. P. Araujo, Yu. G. Pogorelov, P. B. Tavares, J. B. Sousa, and J. M. Vieira, *J. Magn. Magn. Mater.* **242–245**, 655 (2002).

³⁰V. Laukhin, J. Fontcuberta, J. L. Garcia Munoz, and X. Obradors, *Phys. Rev. B* **56**, R10009 (1997).

³¹S. Bhattacharya, A. Banerjee, S. Pal, R. K. Mukherjee, and B. K. Chaudhuri, *J. Phys.: Condens. Matter* **14**, 10221 (2002).